The 12th International Conference of
International Association for Computer Methods and Advances in Geomechanics (IACMAG)
1-6 October, 2008
Goa, India

Presentation of a Homogenized Multi-Phase Model for Reinforced Soil Considering Non-Linear Behavior of Matrix

Ehsan Seyedi Hosseininia
School of Civil Engineering, Faculty of Engineering, University of Tehran, Tehran, Iran

Orang Farzaneh
School of Civil Engineering, Faculty of Engineering, University of Tehran, Tehran, Iran

Keywords: Multi-phase model, homogenization, reinforced soil

ABSTRACT: The multi-phase model for the simulation of reinforced soils is developed by considering the non-linear elastoplastic behaviour of the soil. In this method, it is assumed that both the soil and the reinforcement occupy all over the medium. The reinforcements are placed horizontally among the soil medium. These two phases are connected with each other through a perfect bonding interface. The soil behavior is defined in the frame of being non-linear as a function of stress level considering the distance from the current stress state to the ultimate value as well as the soil stiffness, while the reinforcement which is a linear element, has an elastic-perfectly plastic behavior. In this paper, the formulation of a reinforced soil composite in a triaxial compression test will be explained and the effects of the reinforced characteristics (stiffness and strength) on the behavior of reinforced soil are studied.

1 Introduction

It is for many years that simple methods such as conventional Rankin and Coulomb earth pressure theories are being used to carry out analysis and design of reinforced soil walls and structures. These methods are limit equilibrium approaches that are only applicable for finding and controlling the failure mechanism and they do not concern the deformation induced during and after the failure. Numerical methods hold premise as a design and research tool to investigate the behavior of reinforced soil structures. In addition, they are able to help us to implement parametric studies regarding the geometry or different material types. However, the challenge in numerical simulation of reinforced soils structures is to minimize the calculation time while simulating the structure. It would be a huge barrier when it should be used an advanced constitutive model of the soil for a reinforced soil structure. This is the most reason why there have some attempts to treat or model the reinforced soil structures as a homogenous medium. There are several theoretical works and attempts to predict the essential features governing the behavior of inclusion-reinforced materials as a homogenized material. Considering the deformational analysis, the soil and reinforcements were both regarded as isotopic elastic materials (Harrison and Gerard, 1972, Romstad et al., 1976, Herrmann et al., 1984, Abramento and Whittle, 1993). These works did not respect for the ultimate strength of the composite, though. Other attempts were performed for stability analysis of a reinforced soil structures by applying plasticity in homogenization methods within the framework of yield design theory (de Buhan et al., 1989, Abdi et al. 1994, Mikhaolowski and Zhao, 1995, Anthonie, 1989). However, deformational characteristics of the medium were neglected. In all the above studies, the soil and reinforcing elements are assumed to be bonded to each other without any detachment. None of the aforementioned studies paid attention to the mobilized strength and deformation variation during loading. Referring to homogenization theory for periodic media, a new approach has been recently introduced by Sudret & de Buhan (1999). In this approach, the composite material is regarded as a multiphase system under the hypothesis of perfect bonding between the phases. This macroscopic multiphase material consists of (N+1) phases, i.e. matrix and N directional groups of reinforcement, distributed all over the medium. In the first presented formulation, the constituents were considered as elastic perfectly plastic materials. This was the case where the aim was to expose the ability of the model to consider the hardening behavior of the composite material (de Buhan & Sudret, 1999). This was very important since previous homogenized models could not show this phenomenon in the formulations (Greuell et al., 1994; Bernaud et al., 1995). The feasibility of the application of the introduced formula has been already demonstrated. However, regarding the behavior of the matrix (soil), it is obvious that the composite material have a complex behavior relating to several factors such as confining pressure, density, fabric and stress path in comparison with non-geomaterials such as metal. Also, the elastic strain of the soil, as a particulate medium, is very small say in the order of 10^{-6} since the larger portion of soil strain is of the irreversible type. On the other hand, disregarding the elastic or plastic behavior, the stress-strain relationship of soils is intrinsically nonlinear. It would be, thus, far from the reality when this complicated behavior of soil is neglected while the geotechnical problems are to solve specifically deformation problems (Brinkgreve, 2005) specifically the plastic and residual strains and deformations.

There are a number of soil constitutive models in different frameworks considering the elastic-plastic behavior. In this paper, hypoplasticity concept is considered for the soil behavior and a constitutive model is introduced for reinforced soil in drained condition as a homogenized material in a triaxial space using the multi-phase technique.

2 Principles of multiphase medium

Consider a triaxial reinforced sand sample according to Figure 1, in which the reinforcements are only placed horizontally. Regarding the statics of this two–phase material, the global stress tensor (Σ) can be split into partial stresses corresponding to each phase:

$$\Sigma_1 = \sigma_1^m \ \ , \ \Sigma_3 = \sigma_3^m + \sigma^{inc} \tag{1}$$

where σ^m and σ^{inc} correspond to the stresses macroscopic phases including matrix (soil) and the inclusion (reinforcement). Note that $\Sigma_2=\Sigma_3$ in the triaxial space and for simplicity, the relations are only stated hereafter based on Σ_3 and σ^m_3 .This is the same for the strains mentioned later. It is also important to note that each of these partial stress components be not only the function of the total implied stress on the composite (Σ), but also the function of a couple of self-equilibrated stresses (ρ^m, ρ^r) generated in each phase due to the strain compatibility (Eq. 3). Therefore:

$$\sigma_3^m = L^m \Sigma_3 + \rho^m \ \ , \ \ \sigma^{inc} = L^{inc}\Sigma_3 + \rho^r \tag{2}$$

where $\rho^m+\rho^{inc}=0$ and L^m and L^{inc} are the multipliers being a function of the elastic stiffness of each phase ($L^m+L^{inc}=1$). According to de Buhan & Sudret (1999), this is the stress-like term ρ^i that justifies a hardening behavior in the global behavior of the composite material.

Owing to the hypothesis of perfect bonding between the matrix and the inclusion phases, the strain compatibility is expressed in the following way:

$$\in_1 = \varepsilon_1^m \ \ , \ \in_2 = \varepsilon_2^m = \varepsilon^{inc} \ \ , \ \in_3 = \varepsilon_3^m = \varepsilon^{inc} \tag{3}$$

where ε^m represents the strain in the matrix and ε^{inc} the radial strain of the inclusion. The global strain of the composite $(\in)$ can be thus defined in terms of that of the matrix.

In a multiphase material, each phase of the medium satisfies their own yield criterion which defines the start of the plastic strains in the correspondent phase. The yield function of each constituent in a two-phase system is expressed in the terms of stresses of the medium as follows:

$$f^m[\sigma^m(\Sigma,\rho^m)] \le 0 \ \ for \ \ matrix \ \ , \ \ f^{inc}[\sigma^{inc}(\Sigma,\rho^{inc})] \le 0 \ \ for \ \ inclusion \tag{4}$$

If $f^i<0$, the material has only elastic deformation, but the plastic strains comes into existence when $f^i = 0$. The yield condition is stated as the combination of all phases' yield functions and will be equal to the either of the criteria who goes to become first satisfied (de Buhan & Sudret, 1999). In the presence of a two phases beside each other, the following term is introduced as the global yield criterion for the composite:

$$F(\Sigma,\rho) = Max\left[\, f^m(\sigma^m), f^{inc}(\sigma^{inc}) \right] \le 0 \tag{5}$$

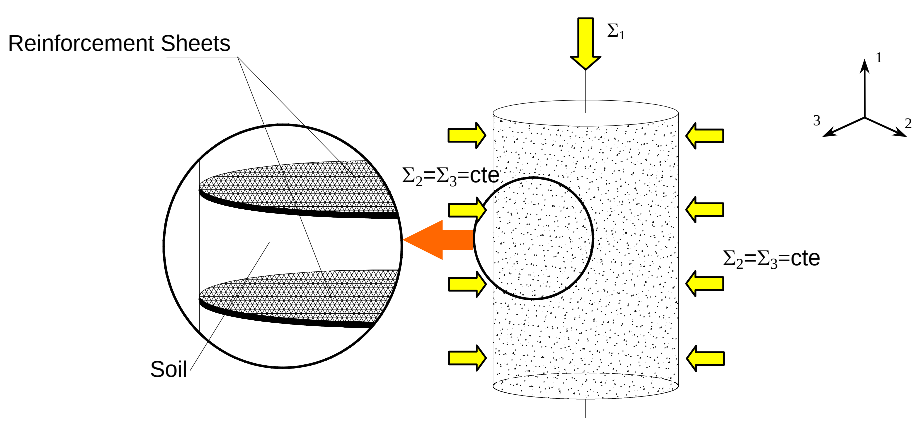

Figure 1. Presentation of decomposition of soil and reinforcements in the reinforced soil composite

2.1 Reinforcement behavior

The reinforcement phase is assumed to have a linear elastic – perfectly plastic tensile behavior with a Young modulus (E^r) and ultimate strength (σ^r_0). The stress-strain relationship for the inclusion is, thus, presented as follows:

$$\sigma^{inc} = E^{inc}\varepsilon^{inc} = E^{inc}\varepsilon_3 \tag{6}$$

where E^{inc} is the inclusion stiffness. The yield function of the inclusion is the linear form of Mises type:

$$f^{inc}(\sigma^{inc}) = \sigma^{inc} - \sigma_0^{inc} \le 0 \tag{7}$$

where σ^{inc}_0 is the ultimate stress in the inclusion which is calculated as ultimate strength in the reinforcement multiplied by its volume fraction (χ):

$$\sigma_0^{inc} = \chi\sigma_0^r \tag{8}$$

And similarly, the inclusion stiffness will be determined as follows:

$$E^{inc} = \chi E^r \tag{9}$$

2.2 Soil constitutive behavior

Supposing that the soil be only failed in the shear mode, the Mohr-Coulomb criterion can be counted on as a yield surface. In principal stress space, the equation of Mohr-Coulomb surface is expressed as follows:

$$f\left(\sigma_1^m,\sigma_3^m\right) = \sigma_1^m - \sigma_3^m - \sin(\varphi_m)\left(\sigma_1^m + \sigma_3^m + \frac{c}{\tan(\varphi_m)}\right) = 0 \tag{10}$$

where c and φ_m are the apparent cohesion and mobilized angle of friction, respectively. In the case of sand, the apparent cohesion is negligible (c=0). In fact, it is assumed that the plastic behavior of the soil starts from the onset of loading, along with elastic deformation, by mobilizing the friction angle which can be considered as a hardening parameter.
For the elastic strain part of the soil, the incremental form of Hooke's law is considered in the triaxial space ($\sigma^m_2 = \sigma^m_3$) as follows:

$$\dot{\varepsilon}_1^m = \frac{1}{E^m}\left[\dot{\sigma}_1^m - 2\upsilon\dot{\sigma}_3^m\right] \quad , \quad \dot{\varepsilon}_3^m = \frac{1}{E^m}\left[-\upsilon\dot{\sigma}_1^m + (1-\upsilon)\dot{\sigma}_3^m\right] \tag{11}$$

where ν and E^m are the soil Poisson's ratio and tangential Modulus, respectively. The following relationship is considered for E^m to be varied with the lateral confining pressure (σ^m_3):

$$E^m = E_0^m\left(\frac{\sigma_3^m}{p'_0}\right)^{\alpha} \tag{12}$$

E^m_0 is the reference Young modulus and α is a positive model constants and p'_0 is the reference pressure (equals to the atmospheric pressure = 101 kPa).
The unit vector (**n**) normal to the yield surface is assessed by differentiating equation (10) with respect to the principal stresses as well as holding **n** : **n** = 1 in the following way:

$$n_1 = \frac{1-\sin(\varphi_m)}{\sqrt{2(1+\sin^2(\varphi_m))}} \quad , \quad n_2 = 0 \quad , \quad n_3 = \frac{-(1+\sin(\varphi_m))}{\sqrt{2(1+\sin^2(\varphi_m))}} \tag{13}$$

The symbol : denotes the scalar product of two tensors. The direction of the incremental plastic strain rate (**m**) can be defined similarly to (**n**) as follows:

$$m_1 = \frac{1-\sin(\psi)}{\sqrt{2(1+\sin^2(\psi))}} \quad , \quad m_2 = 0 \quad , \quad m_3 = \frac{-(1+\sin(\psi))}{\sqrt{2(1+\sin^2(\psi))}} \tag{14}$$

where ψ is the dilation angle of the soil. It is reminded that the vector (**m**) is normalized too by enforcing **m** : **m** = 1. Consequently, the plastic strain rate can be defined from the following flow rule:

$$\dot{\varepsilon}_{p\,i}^m = <\lambda> m_i \quad i = 1,3 \tag{15}$$

Where the McCauley brackets < > defines the function < x > = x if x > 0 and < x > = 0 otherwise. λ is the loading index and is introduced as follows:

$$\lambda = \frac{1}{h}\left(\dot{\sigma}_i^m : n_i\right) \tag{16}$$

where h is the plastic modulus and demonstrates the distance from current stress level to the bounding (ultimate) surface in the framework of hypoplasticity (Dafalias, 1986):

$$h = h_0\left[\sin(\phi_f) - \sin(\varphi_m)\right]^\beta \tag{17}$$

h_0 and β are model parameters and Φ_f is the ultimate mobilized friction angle of soil. Combining the elastic and plastic strain rate portions, the incremental stress-strain of the soil can be assessed in the following form:

$$\dot{\varepsilon}_1^m = C_1\,\dot{\sigma}_1^m + C_2\,\dot{\sigma}_3^m \quad , \quad \dot{\varepsilon}_3^m = C_3\,\dot{\sigma}_1^m + C_4\,\dot{\sigma}_3^m \tag{18}$$

where:

$$C_1 = \frac{1}{E^m} + \frac{1}{h}(m_1 n_1) \quad , \quad C_2 = \frac{-2\upsilon}{E^m} + \frac{1}{h}(m_1 n_3)$$
$$C_3 = \frac{-\upsilon}{E^m} + \frac{1}{h}(m_3 n_1) \quad , \quad C_4 = \frac{1-\upsilon}{E^m} + \frac{1}{h}(m_3 n_3) \tag{19}$$

3 Constitutive behavior of the composite material

In accordance with Eq. 5 and 10, the yield criterion of the matrix dominates to be the defined as global yield criterion of the composite in the following way:

$$F(\Sigma, \rho) = f^m\left(\Sigma, \sigma^{inc}\right) = 0 \tag{20}$$

Since there is no reinforcement in the 1-1 axis and the confining pressure imposed on the sample is constant during the test, the global stresses can be expressed in terms of partial stresses as follows:

$$\dot{\sigma}_1^m = \dot{\Sigma}_1 \quad , \quad \dot{\sigma}_3^m = -\dot{\sigma}^{inc} \tag{21}$$

Based on strain compatibility in accordance with Eq. 3, the matrix strain rate equals to the composite strain rate. Applying Eq. 20 in Eq. 18 as well as considering Eq. 6, the stress-strain relationship of the composite material is assessed as follows:

$$\begin{Bmatrix} \dot{\epsilon}_1 \\ \dot{\epsilon}_3 \end{Bmatrix} = \begin{bmatrix} C_1^H & C_2^H \\ C_3^H & C_4^H \end{bmatrix} \begin{Bmatrix} \dot{\Sigma}_1 \\ \dot{\sigma}^{inc} \end{Bmatrix} \tag{22}$$

with:

$$C_1^H = \frac{C_4}{C_1C_4 - C_2C_3} \quad , \quad C_2^H = \frac{-C_2}{C_1C_4 - C_2C_3} \quad , \quad C_3^H = 0 \quad , \quad C_4^H = E^{inc} \tag{23}$$

4 Simulation by the model

As can be figured out from the assessment of the constitutive relations of the composite material, only the parameters of two components (soil and reinforcement) are involved in the formulations. In this part, the aim is to model the behavior of triaxial sandy sample which is reinforced by three horizontal layers of reinforcing sheets placed with the same distance. The triaxial sample has a diameter of 38 mm and 76 cm high. Table 1 shows the characteristics of two reinforcement types (R1 and R2) used in the simulations presented in this section. The radial Young modulus (E^r) is calculated for reinforcements with assumption of being linear with an ultimate tensile strength (F^r_{ult}). Referring to the thickness of the whole sheets and the height of the sample, the volume ratio (χ) equals to 3(0.2)/76=0.8%.

Table 1. Properties of the reinforcements

Reinforcement type	t [mm]	Rupture Strain [%]	F^r_{ult} [kN/m]	E^r [MPa]
R1	0.5	8.0	30.0	120
R2	0.5	6.0	50.0	60

Regarding the soil parameters, they are divided into three groups including elastic, dilatancy and hardening parameters. It is supposed that the sand state is dense with a dilation angle 12.5^o. The values of these parameters are shown in Table 2 for typical sand with Φ_f = 40^o.

Table 2. Model parameters for sand

Elastic			Dilatancy	Hardening		
E^m_0 [kPa]	α [-]	ν [-]	ψ [degree]	h_0 [kPa]	β [-]	Φ_f [degree]
20000	0.5	0.2	12.5	E^m	1	40

Figure 3 shows the variation of stress ratio and volumetric strain of the different sandy samples (non-reinforced and reinforced) along the axial strain. As can be seen, the mobilized strength of non-reinforced sample (NR) increases non-linearly with the axial strain and then it reaches the ultimate value which rests constant. However, this is not the case for the reinforced samples; there is no ultimate value for the composite material until the axial strain of 20%. Although the initial stress-strain relationship of the composite samples coincide with that of the NR sample in small axial strains (smaller than 2%), the slope of the curves deviates from each other. Two different reasons provoke this behavior. First, the soil stiffness augments along with the increase in the confining pressure due to the existence of the reinforcement (also see Figure 4). Secondly, the reinforcement stiffness plays his specific role itself in the global deformational behavior. Comparing the E^r of the reinforcements, it can be concluded that the overall stiffness of the composite is larger with the stiffer reinforcement. Regarding the deformational behavior, according to Figure 3(b), the reinforcement prevents the system to have dilative behavior. In other words, the more the reinforcement is stiff, the less the reinforced soil dilates. This phenomenon is clearly observed in the experimental tests performed in the laboratory (e.g., Broms, 1977; Chandrasekaran et al., 1989; Haeri et al., 2000).

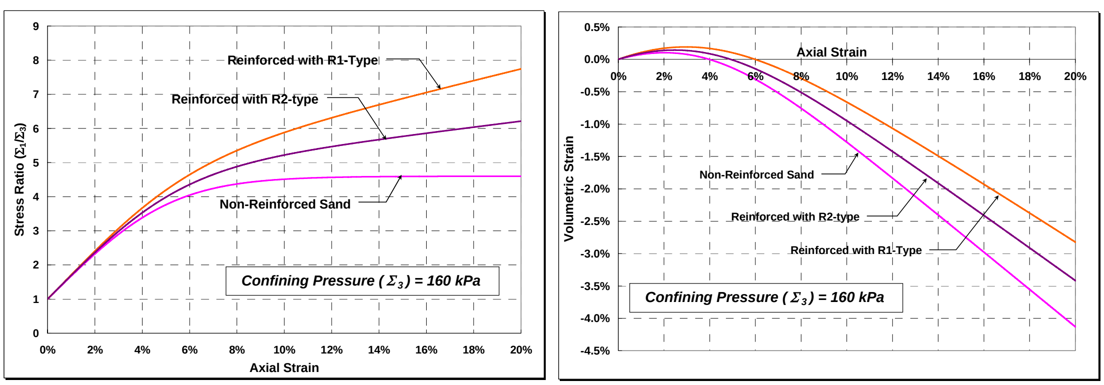

(a) (b)

Figure 3. Variation of stress ratio and volumetric strain versus axial strain for non-reinforced and sand samples reinforced by R1-Type and R2-Type under the confining pressure level of 160 kPa

To understand the effect of confining pressure level on the behavior of composite reinforced system, the variation of stress ratio and volumetric strain along axial strain for R2-type reinforced sand samples are modelled in Figure 4 under confining pressure levels of 20 kPa and 160 kPa. As seen, for the same reinforcement properties, the sample with low confining pressure (=20 kPa) experiences large growth in strength and less dilative deformation in comparison with the sample with high confining pressure (=160 kPa).
A parametric study is performed to find the influence of the soil stiffness on the composite stiffness. In the present model, according to Eq. 12, the soil deformation modulus is defined as a function of applied confining pressure (σ^m_3). Thus, when the sample is under loading, the confining pressure increases by the reinforcement effect due to the resistance against the lateral deformation and thus the soil stiffness augments. In order to find the portion of confining pressure dependency in the behavior of the composite, the soil modulus holds constant and equals to the initial value in the other series of modellings as shown in Figure 4. It can be found that both strength and volumetric strain values are affected by the behavior of confining pressure dependency especially in low levels of confining pressure. The model dependant to the actual confining pressure in the reinforced system demonstrates more strength and high degree of dilatancy.

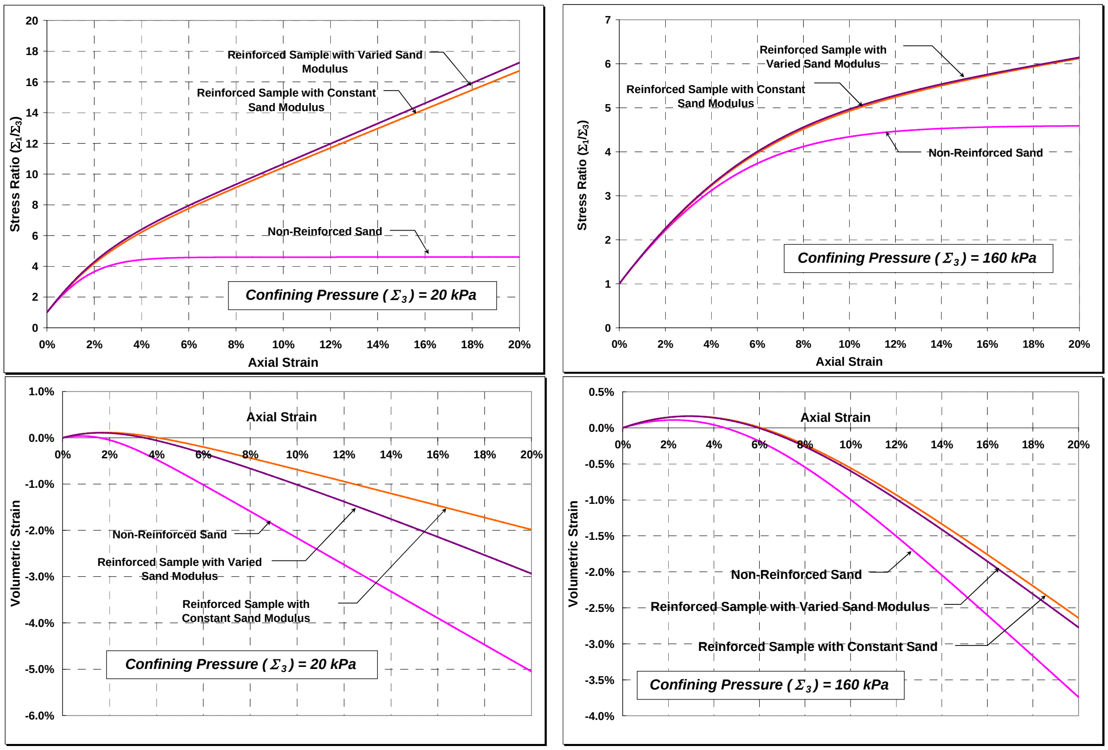

(a) (b)

Figure 4. Variation of stress ratio and volumetric strain versus axial strain for non-reinforced and reinforced sand samples with R2-Type under confining pressure levels of (a) 20 kPa; (b) 160 kPa.

Applying different confining pressures on the reinforced sand sample, the variation of stress ratio and volumetric strain along the axial strain are plotted in Figure 5 for both types of reinforcements. As can be seen, the composite shows a well suited non-linear behavior from the beginning of loading, which is more dominant in lower confining pressures. The reinforcement stress does not reach the ultimate strength in none of the samples. Also, it can be seen that in the tests with higher confining pressure, there is a weak tendency in the growth of the composite strength, while in lower confining pressures, the strength augments sharply, and consequently, it could be guessed that there would be a big fall in strength after reaching the maximum value. The same results are already stated by McGown et al. (1978) and Haeri et al. (2000) who have performed several triaxial and plane strain tests on reinforced samples, respectively. As the other effect of confining pressure level and its relationship with different types of reinforcements, it can be seen that the larger the confining pressure is, the less the stiffness of the reinforcement has an increasing effect in the strength. Regarding two reinforcement types, in spite of big differences in stress ratios for various confining pressures, the volumetric strain has less sensitivity. In any event, as stated before, the reinforcement with bigger stiffness (R1) enforces the sample to behave more contractively, as stated by Tatsuoka and Yamauchi (1986), and this effect is more evident for lower confining pressures. According to Table 2, although the stiffness of R2 is twice than that of R1 and different stress-strain behavior can be distinguished, no significant change can be found in the volumetric strain values of these two samples. However, the behavior goes to be more contractive with increase in confining pressure.

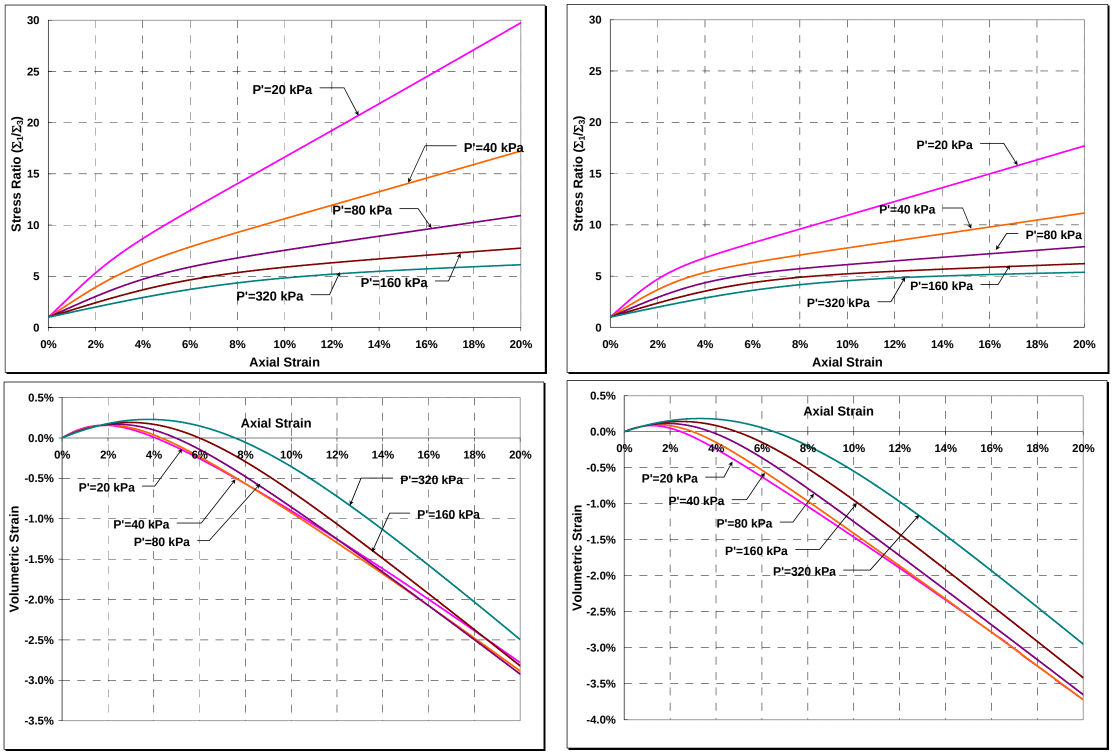

(a) (b)

Figure 5. Stress ratio and volumetric strain versus axial strain with different confining pressures (P') for sandy samples reinforced by: (a) reinforcement Type R1; (a) reinforcement Type R2

5 Summary and conclusion

In this paper, a comprehensive constitutive model of reinforced sand sample, with the concept of multiphase formulation, is introduced for compression triaxial test under drained condition. The multiphase model presented by de Buhan and Sudret (1999) is developed by improving the soil model in the framework of bounding surface and hypoplasticity which imposes non-linear behavior and thus can simulate the plastic deformation under various monotonic loading conditions. Within the multiphase concept and considering the reinforced soil as a homogenized material, the reinforcement phase is supposed to be located all over the medium with the soil through a perfect bonding in the horizontal direction and hence constituting an anisotropic medium. This procedure can help us to model the behavior of a composite material by combining the characteristics of each component in the system.

Introducing two reinforcement types with different stiffness, the behavior of reinforced samples are compared with that of the non-reinforced sample. Also, the influence of implied inter-confining pressure in the soil on the increase of the composite strength and volumetric deformation was investigated. At the end, several simulations for two reinforced sand samples with different types of reinforcements are presented under different confining pressures and the variation of stress ratio and volumetric stains are discussed. It showed that reinforcing the sand samples with inclusions have great effect in low confining pressures. It is demonstrated that the model can simulate appropriately the reinforced soil behavior regarding the composite stress–strain including the variation of global stiffness, strength and the volumetric deformation. It is also pointed out that the simulation results agree well with the observations obtained in the experimental laboratory tests.

6 References

Abdi R., de Buhan P., Pastor J. 1994. Calculation of the critical height of a homogenized reinforced soil wall: a numerical approach. *Int. J. for Numerical and analytical methods in Geomechanics.* **18**, 485-505.

Abramento M., Whittle A. J. 1993. Shear-lag analysis of planar soil reinforcement in plane-strain compression. *J. of Engineering*

Mechanics. ASCE, **119**(2), 270-291.

Anthoine A., 1989. Mixed modeling of reinforced soils within the framework of the yield design theory. *Computers and Geotechnics*, **7**, 67-82.

Bernaud D., de Buhan P., Maghous S. 1995. Numerical simulation of the convergence of a bolt-supported tunnel through a homogenization method. *Int. J. Num. Met. Geo.*, **19**, 267-288.

Brinkgreve R.B.J. 2005. Selection of Soil Models and Parameters for Geotechnical Engineering Application. *Soil Constitutive Models: Evaluation, Selection, and Calibration*, Geotechnical Special Publication No. 128, 69-98.

Chandrasekaran B., Broms B.B., Wong K.S. 1989. Strenght of fabric reinforced sand under axisymetric loading. Geotextiles and Geomembranes, **8**, 293-310.

Dafalias Y. F. 1986. Bounding surface plasticity, I: mathematical foundation and hypoplasticity. *J. of Engineering mechanics*, ASCE, **112**(12), 1263-1291.

de Buhan P., Mangiavacchi R., Nova R., Pellegrini G., Salençon, J. 1989. Yield design of reinforced earth walls by a homogenization method. *Géotechnique*, **39**(2), 189-203.

de Buhan P., Sudret, B. 1999. A two-phase elastoplastic model for unidirectionally-reinforced materials. *Eur. J. Mech. A/Solids*, **18**, 995-1012.

Greuell E., de Buhan P., Panet P., Salençon, J. 1994. Behavior of tunnels reinforced by untentioned bolts. 13th Int. Conference on Soil Mechanics and Foundations Engineering. Oxford and IBH Pub., 869-872.

Haeri S.M., Noorzad R., Oskoorouchi A.M. 2000. Effect of geotextiles reinforcement on the mechanical behavior of sand. *Geotextiles and Geomembranes*, 18, 385-402.

Harrison W.J., Gerrard C. M. 1972. Elastic theory applied to reinforced earth. *J. of Soil Mechanics and Foundations Division*, ASCE, **98**(12), 1325-1345.

Herrmann L.R., Welch K.R., Berg, R.R. 1984. Composite FEM analysis for layered systems. *J. of Engineering Mechanics*, ASCE **110**(9), 1284-1302.

McGown A., Andrawes K. Z. and Hasani M. M. 1978. Effect of inclusion properties on the behavior of sands. *Géotechnique* **3**(28), 327-346.

Michalowski R.L., Zhao, A. 1995. Continuum versus structural approach to stability of reinforced soil. *J. of Geotechnical Engineering*. ASCE, **121**, 152-162.

Romtad K.M., Herrmann L.R., Shen C.K. 1976. Integrated study of reinforced earth-II: Behavior and design. *J. Geotech. Eng. Div.*, ASCE **102**(6), 577-590.

Sudret B., de Buhan P. 1999. Modélisation multiphasique de matériaux renforcés par inclusions linéaires. *C. R. Acad. Sci*. Paris Serie II-b 327, 7-12.

Tatsuoka F., Yamauchi H. 1986. A reinforcing method for steep clay slopes with non-woven fabric. Geotextiles and Geomembranes, **4**(3/4), 241-268.

The paper may be considered for
(Please indicate your choice by putting √ in the appropriate box)

1. Oral Presentation	√
2. Poster Session	